arXiv:2205.13341v1 [cs.LG] 26 May 2022

QUIC-FL: Quick Unbiased Compression for Federated Learning

Ran Ben Basat *
University College London
r.benbasat@ucl.ac.uk

Shay Vargaftik *
VMware Research
shayv@vmware.com

Amit Portnoy *
Ben-Gurion University
amitport@post.bgu.ac.il

Gil Einziger
Ben-Gurion University
gilein@bgu.ac.il

Yaniv Ben-Itzhak
VMware Research
ybenitzhak@vmware.com

Michael Mitzenmacher
Harvard University
michaelm@eecs.harvard.edu

Abstract

Distributed Mean Estimation (DME) is a fundamental building block in communication efficient federated learning. In DME, clients communicate their lossily compressed gradients to the parameter server, which estimates the average and updates the model. State of the art DME techniques apply either unbiased quantization methods, resulting in large estimation errors, or biased quantization methods, where unbiasing the result requires that the server decodes each gradient individually, which markedly slows the aggregation time. In this paper, we propose QUIC-FL, a DME algorithm that achieves the best of all worlds. QUIC-FL is unbiased, offers fast aggregation time, and is competitive with the most accurate (slow aggregation) DME techniques. To achieve this, we formalize the problem in a novel way that allows us to use standard solvers to design near-optimal unbiased quantization schemes.

1 Introduction

In federated learning [1, 2], clients periodically send their gradients to the parameter server, which calculates their means. This communication is often a network bottleneck, and methods to approximate the mean using small communication are desirable. The Distributed Mean Estimation problem (DME) [3] formalizes this fundamental building block as follows: each of n *clients* communicate a representation of a d-dimensional vector to a *parameter server* which estimates the vectors' mean.

Various DME methods have been studied (e.g., [3, 4, 5, 6, 7]), examining tradeoffs between the required bandwidth and performance metrics such as the estimation accuracy, learning speed, and the eventual accuracy of the model. These works utilize lossy compression techniques, using only a small number of bits per coordinate, which is shown to accelerate the training process [8, 9]. For example, in [3], each client randomly rotates its vector before applying stochastic quantization. When receiving the messages from the clients, the server sums up the estimates of the rotated vectors and applies the inverse rotation. As the largest coordinates are asymptotically larger than the mean, their Normalized Mean Squared Error ($NMSE$) is bounded by $O\left(\log d/n\right)$. They also propose an entropy encoding method that reduces the $NMSE$ to $O(1/n)$ but is slow and not GPU-friendly. A different approach to DME computes the Kashin's representation [10] of a client's vector before applying quantization [11, 12]. Intuitively, this replaces the input d-dimensional vector by $\lambda \cdot d$ coefficients, for some $\lambda > 1$, each bounded by $O\left(\sqrt{\|x\|_2/d}\right)$. Applying quantization to the coefficients instead of the original vectors allows the server to estimate the mean using $\lambda > 1$ bits per coordinate with an $NMSE$ of $O\left(\frac{\lambda^2}{(\sqrt{\lambda}-1)^4 \cdot n}\right)$. However, it requires applying multiple randomized Hadamard transforms, slowing down its encoding.

*Equal Contribution.

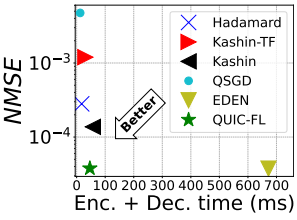
Preprint. Under review.

Algorithm	QSGD [14]	Hadamard [3]	Kashin [11, 12]	EDEN [7]	QUIC-FL (Ours)
Encoding complexity	$O(d)$	$O(d \cdot \log d)$	$O(d \cdot \log d \cdot \log(n \cdot d))$	$O(d \cdot \log d)$	$O(d \cdot \log d)$
Decoding complexity	$O(n \cdot d)$	$O(n \cdot d + d \cdot \log d)$	$O(n \cdot d + d \cdot \log d)$	$O(n \cdot d \cdot \log d)$	$O(n \cdot d + d \cdot \log d)$
NMSE	$O(d/n)$	$O(\log d/n)$	$O(1/n)$	$O(1/n)$	$O(1/n)$

Table 1: The asymptotic guarantees of the algorithms with $b = O(1)$ bits per coordinate and using the Hadamard transform for rotation based algorithms. The table does not consider variable length encodings (see Appendix A).

The recently introduced DRIVE [5] (which uses $b = 1$ bits per coordinate) and its generalization EDEN [7] (that can be used with any $b > 0$) also randomly rotate the input vector, but unlike [3] use *biased* and deterministic quantization on the rotated coordinates. Interestingly, both yield *unbiased* estimates of the original vector after multiplying the estimated vector by a real-valued "scale" that is sent by each client together with the quantization. Both solutions have an $NMSE$ of $O(1/n)$ and are empirically more accurate than Kashin's representation. However, to achieve unbiasedness, each client must generate a distinct rotation matrix independently from other clients. In turn, the server must invert the rotation for each vector before aggregating them, resulting in $O(n)$ rotations instead of one, asymptotically increasing the decoding time.

In this work we present **Q**uick **U**nbi**a**sed **C**ompression for **F**ederated **L**earning (QUIC-FL): a DME algorithm that produces unbiased estimates, with a fast estimation procedure and an NMSE of $O\left(1/n\right)$. QUIC-FL also leverages random rotations, and uses the observation that after rotation the coordinates' distribution approaches d i.i.d. normal variables, $\mathcal{N}\left(0, \|x\|_2/d\right)$ [5]. The goal of QUIC-FL is to unbiasedly quantize each coordinate while minimizing the error. Compared with [3], we present two key improvements: (1) Instead of quantizing all coordinates, we allow the algorithm to send an expected p-fraction of the *rotated* coordinates exactly (up to precision) for some small p (e.g., $p = 1/512$). This limits the range of the other coordinates to $[-T_p, T_p]$, where $T_p = O(1)$ for any constant $p > 0$, thus reducing the possible quantization error significantly. (2) We study how to leverage *client-specific shared randomness* [13] to reduce the error further. Specifically, we model the problem of transmitting a "truncated" normal random variable $Z \sim \mathcal{N}(0, 1) \mid Z \in [-T_p, T_p]$, using $b \in \mathbb{N}^+$ bits, with the goal of obtaining an unbiased estimate at the server. Our model considers both a client's private randomness and shared randomness, allowing us to derive an input to optimization problem solver, whose output yields algorithms with a near-optimal accuracy to bandwidth tradeoff.



We implement QUIC-FL in PyTorch [15] and TensorFlow [16], showing that it can compress vectors with over 33 million coordinates within 44 milliseconds and is markedly more accurate than existing fast-estimate approaches such as QSGD [14], Hadamard [3], and Kashin [11, 12]. Compared with DRIVE [5] and EDEN [7], QUIC-FL has only slightly worse NMSE (e.g., less than 1% for $b = 4$ bits per dimension) while asymptotically improving the estimation time, as shown on the right. The figure illustrates the cycle (encode plus decode) times vs. NMSE for $b = 4$ bits per coordinate, $d = 2^{20}$ dimensions, and $n = 256$ clients. (see §4 for the algorithms' description.) We summarize the asymptotic guarantees of the discussed DME techniques in Table 1.

While we have surveyed the most relevant related work, we review other techniques in Appendix A.

2 Preliminaries

Problems and Metrics. Given a non-zero vector $x \in \mathbb{R}^d$, a vector compression protocol consists of a client that computes a message X and a server that given the message estimates $\widehat{x} \in \mathbb{R}^d$. The *vector Normalized Mean Squared Error* ($vNMSE$) of the protocol is defined as $\frac{\mathbb{E}\left[\|x-\widehat{x}\|_2^2\right]}{\|x\|_2^2}$ [5, 7].

This problem generalizes to the Distributed Mean Estimation (DME) problem, where n clients have vectors $\left\{x_c \in \mathbb{R}^d\right\}$ that they communicate to a centeralized server. We are then interested in minimizing the *Normalized Mean Squared Error* ($NMSE$), defined as $\frac{\mathbb{E}\left[\left\|\frac{1}{n}\sum_{c=1}^n \widehat{x}_c - \frac{1}{n}\sum_{c=1}^n x_c\right\|_2^2\right]}{\frac{1}{n}\cdot\sum_{c=1}^n \|x_c\|_2^2}$ [3, 5, 7]. Note that for unbiased algorithms and independent estimates, we have that $NMSE = vNMSE/n$ [5].

Shared randomness. We allow both global (common to all clients and the server) and client-specific shared randomness (common to a single client and the server).

3 The QUIC-FL Algorithm

3.1 Rotation-based Truncated Quantization

Similarly to previous works [3, 5, 7], our algorithm uses random rotations after which the coordinates' distribution approaches independent normal random variables for high dimensions [5]. QUIC-FL features near-optimal *unbiased* quantization for the normal distribution. We emphasize that QUIC-FL is unbiased for any input; its quantization is just tuned for normally distributed inputs. The most closely related previous works, DRIVE [5] and EDEN [7], can achieve unbiased results, but only by using a distinct rotation matrix for each client. QUIC-FL instead allows all clients to use *the same* rotation matrix (generated with global shared randomness). QUIC-FL's unbiasedness is guaranteed by its quantization technique that uses both private randomness and client-specific shared randomness (shared between it and the server). As all clients apply the same rotation matrix, the server can sum the *rotated* vectors and apply a single inverse rotation, speeding up the aggregation.

As another comparison point, [3], given a bit budget of $b(1+o(1))$ bits per packet, stochastically quantizes each rotated coordinate into one of 2^b levels. The algorithm uses a max-min normalization, and the levels are uniformly spaced between the minimal and maximal coordinates. Their algorithm then communicates the max and min, together with b bits per coordinate indicating its quantized level, and is shown to have a $NMSE$ of $O\left(\log d/n\right)$ for any $b=O(1)$. QUIC-FL has two main improvements over [3]. The first uses a conceptually simple modification that truncates the rotated coordinates' distribution. This is achieved by allowing the algorithm to send a p fraction (e.g., for $p=\frac{1}{512}$) of the coordinates precisely, thereby reducing the $NMSE$ to $O\left(1/n\right)$. The second leverages client-specific shared randomness to lower the $NMSE$ further.

We begin by analyzing the value of the truncation. Let $Z=\mathcal{N}(0,1)$ be a normal random variable, modeling a rotated (and scaled) coordinate. Given a user-defined parameter p, we can compute a threshold T_p such that $\Pr\left[Z\notin\left[-T_p,T_p\right]\right]=p$. For example, by picking $p=2^{-9}$ (i.e., less than 0.2%), we get a threshold of $T_p\approx 3.097$.[2]

In general, for any *constant* $p>0$, we have $T_p=O(1)$, and using b bits for each coordinate in $\left[-T_p,T_p\right]$ we get a $NMSE$ of $O\left(1/n\right)$ for any constant b (due to unbiased and independent quantization among clients). For example, consider sending each coordinate in $\left[-T_p,T_p\right]$ using $b=1$ bit per coordinate. One solution would be to use stochastic quantization, i.e., given a coordinate $Z\in\left[-T_p,T_p\right]$ send T_p with probability $\frac{Z+T_p}{2T_p}$ and $-T_p$ otherwise. This quantization results in an expected squared error of

$$\mathbb{E}\left[(Z-\widehat{Z})^2\right]=\frac{1}{\sqrt{2\pi}}\int_{-T_p}^{T_p}\left(\frac{z+T_p}{2T_p}\cdot(z-T_p)^2+\frac{T_p-z}{2T_p}\cdot(z+T_p)^2\right)\cdot e^{-\frac{z^2}{2}}dz.$$

With $p{=}2^{-9}$ as above, we get $\mathbb{E}\left[(Z-\widehat{Z})^2\right]{\approx}8.58$. As shown in Appendix B, for QUIC-FL $vNMSE=\mathbb{E}\left[\left(Z-\widehat{Z}\right)^2\right]+O\left(\sqrt{\frac{\log d}{d}}\right)$. Thus, using the above for each coordinate for large gradients results in $NMSE\approx 8.58/n$. We next show that shared randomness decreases $\mathbb{E}[(Z-\widehat{Z})^2]$ and thus its $NMSE$.

3.2 Client-specific Shared Randomness: Intuition and Examples

We now provide an example to show how shared randomness can improve the $vNMSE$, leading to §3.3 where we formalize our approach to finding near-optimal unbiased compression schemes for truncated $\mathcal{N}(0,1)$ variables. Using a single shared random bit (i.e., $H\in\{0,1\}$), we can use the following algorithm, where X is the sent message and $\alpha=0.8,\beta=5.4$ are constants:

$$X=\begin{cases}1 & \text{if } H=0 \text{ and } Z\geqslant 0\\ 0 & \text{if } H=1 \text{ and } Z<0\\ Bernoulli(\frac{2Z}{\alpha+\beta}) & \text{If } H=1 \text{ and } Z\geqslant 0\\ 1-Bernoulli(\frac{-2Z}{\alpha+\beta}) & \text{If } H=0 \text{ and } Z<0\end{cases}\qquad \widehat{Z}=\begin{cases}-\beta & \text{if } H=X=0\\ -\alpha & \text{if } H=1 \text{ and } X=0\\ \alpha & \text{If } H=0 \text{ and } X=1\\ \beta & \text{If } H=X=1\end{cases}.$$

[2]Note that, because we begin with a normal random variable Z, truncation is effective at removing the long, small-probability tails. Additionally, as the learning process typically uses 16-64 bit floats, and we further need to send the coordinate indices, sending each coordinate is expensive, and thus we focus on small p values.

For example, if $Z = 1$, then with probability $1/2$ we have that $H = 0$ and thus $X = 1$, and otherwise the client sends $X = 1$ with probability $\frac{2}{\alpha+\beta}$ (and otherwise $X = 0$). Similarly, the reconstruction would be $\widehat{Z} = \alpha$ with probability $1/2$ (when $H = 0$), $\widehat{Z} = \beta$ with probability $1/2 \cdot \frac{2}{\alpha+\beta} = 0.16$, and $\widehat{Z} = -\alpha$ with probability $1/2 \cdot \frac{\alpha+\beta-2}{\alpha+\beta} = 0.84$. Indeed, we have that the estimate is unbiased since:

$$\mathbb{E}[\widehat{Z} \mid Z = 1] = \alpha \cdot 1/2 + \beta \cdot 1/2 \cdot \frac{2}{\alpha+\beta} + (-\alpha) \cdot 1/2 \cdot \frac{\alpha+\beta-2}{\alpha+\beta} = 1.$$

We calculate the quantization's expected squared error, conditioned on $Z \in [-T_p, T_p]$. (From symmetry, we integrate over positive t.)

$$\mathbb{E}\left[(Z-\widehat{Z})^2\right] = \sqrt{\frac{2}{\pi}}\left(\int_0^{T_p} \frac{1}{2} \cdot \left((z-\alpha)^2 + \frac{2z}{\alpha+\beta} \cdot (z-\beta)^2 + \frac{\alpha+\beta-2z}{\alpha+\beta} \cdot (z+\alpha)^2\right) \cdot e^{-z^2/2} dz\right)$$

Using the same $p = 2^{-9}$ parameter ($T_p \approx 3.097$), we get an error of $\mathbb{E}\left[(Z-\widehat{Z})^2\right] \approx 3.29$, 61% lower than without shared randomness. This algorithm is derived from the solver, which numerically approximates the optimal unbiased algorithm with a single shared random bit, in terms of expected squared error, for this p. We present our general approach for using the solver in the following sections.

3.3 Designing Near-optimal Unbiased Compression Schemes

In order to design our compression scheme, we first model the problem as follows:

- We first choose a parameter $p > 0$, the expected fraction of coordinates allowed to be sent exactly.
- The input, known to the client, is a coordinate $Z \sim \mathcal{N}(0,1)$. The p parameter restricts further the distribution to $Z \in [-T_p, T_p]$.
- The shared randomness H is known to both the client and server, and without loss of generality, we assume that $H \sim U[0,1]$. We denote by $\mathcal{H} = [0,1]$ the domain of H.
- We use a bit budget of $b \in \mathbb{N}^+$ bits per coordinate, and accordingly assume that the messages are in the set $\mathcal{X}_b = \{0, \ldots, 2^b - 1\}$.[3] Again, coordinates outside the range $[-T_p, T_p]$ are sent exactly.
- The client is modeled as $S : \mathcal{H} \times \mathbb{R} \to \Delta(\mathcal{X}_b)$. That is, the client observes the shared randomness H and the input Z, and chooses a distribution over the messages. We further denote by $S_x(h,z)$ the probability that the client sends $x \in \mathcal{X}_b$ given h and z (i.e., $\forall h, z : \sum_x S_x(h,z) = 1$). For example, it may choose $S_x(0,0) = \begin{cases} 1/2 & \text{If } x \in \{0,1\} \\ 0 & \text{Otherwise} \end{cases}$. That is, the client shall use private randomness to decide whether to send $x = 0$ or $x = 1$, each with probability $1/2$.
- The server is modeled as a function $R : \mathcal{H} \times \mathcal{X}_b \to \mathbb{R}$, such that if the shared randomness is $H \in \mathcal{H}$ and the server receives the message $X \in \mathcal{X}_b$, it produces an estimate $\widehat{Z} = R(H, X)$.
- We require that the estimates are unbiased, i.e., $\mathbb{E}[\widehat{Z} \mid Z] = Z$, where the expectation is taken over both $H \in \mathcal{H}$ and the private randomness of the client.

We are now ready to formally define the problem.

$$\begin{aligned} \underset{S,R}{\text{minimize}} \quad & \frac{1}{\sqrt{2\pi}} \int_{-T}^{T} \int_0^1 \sum_x S_x(h,z) \cdot (z - R(h,x))^2 \cdot e^{-z^2/2} \, dh \, dz \\ \text{subject to} \quad & \int_0^1 \sum_x S_x(h,z) \cdot R(h,x) \, dh = z, \qquad \forall z \in [-T, T]. \end{aligned}$$

We are unaware of methods for solving the above problem analytically. Instead, we propose a discrete relaxation of the problem, allowing us to approach it with a *solver*.[4] Namely, we model the algorithm as an optimization problem and let the solver output the optimal algorithm. To that end, we need to discretize the problem. Specifically, we make the following relaxations:

[3] We note that using entropy encoding, one may use more than 2^b messages (and thereby reduce the error) if the resulting entropy is bounded by b (e.g., [3, 7, 14]). As our goal is to design a quick and GPU-friendly compression scheme, we do not investigate entropy encoding further.

[4] We used the Gekko [17] software package that provides a Python wrapper to the APMonitor [18] environment, running the solvers Interior Point OPTimizer (IPOPT) [19] and Advanced Process OPTimizer (APOPT) [20].

- The shared randomness H is selected uniformly at random from a finite set of values $\mathcal{H}_\ell \triangleq \{0, \ldots, 2^\ell - 1\}$, i.e., using ℓ shared random bits.
- The truncated distribution of a rotated and scaled $Z \sim \mathcal{N}(0,1)$ coordinate is approximated using a finite set of *quantiles* $\mathcal{Q}_m = \{q_0, \ldots, q_{m-1}\}$, for a parameter $m \in \mathbb{N}^+$. In particular, the quantile is the point on the CDF of the truncated normal distribution (restricted to $[-T_p, T_p]$) such that the $\Pr[Z \leqslant q_i \mid Z \in [-T_p, T_p]] = \frac{i}{m-1}$. Notice that we have m such quantiles, corresponding to the probabilities $\left\{0, \frac{1}{m-1}, \frac{2}{m-1}, \ldots, 1\right\}$. For example, $p = 2^{-9}$ and $m = 4$ we get the quantile set $\mathcal{Q}_4 \approx \{-3.097, -0.4298, 0.4298, 3.097\}$.
- The client is now modeled as $S : \mathcal{H}_\ell \times \mathcal{Q}_m \to \Delta(\mathcal{X}_b)$. That is, for each shared randomness $h \in \mathcal{H}_\ell$ and quantile $q \in \mathcal{Q}_m$ values, the client has a *probability distribution* on the messages from which it samples, using private randomness, at encoding time.
- The server is modeled as a function $R : \mathcal{H}_\ell \times \mathcal{X}_b \to \mathbb{R}$, such that if the shared randomness is H and the server receives the message X, it produces an estimate $\widehat{Z} = R(H, X)$.

Given this modeling, we use the following variables:

- $s = \{s_{h,q,x} \mid h \in \mathcal{H}_\ell,\ q \in \mathcal{Q}_m,\ x \in \mathcal{X}_b\}$, where $s_{h,q,x}$ denotes the probability of sending a message x, given the quantile q and shared randomness value h. We note that the solver's solution will only instruct us what to do if all our coordinates were quantiles in $\mathcal{Q}_m$. In what follows, we show how to interpolate the result and get a practical algorithm for any $Z \in [-T_p, T_p]$.
- $r = \{r_{h,x} \mid h \in \mathcal{H}_\ell,\ x \in \mathcal{X}_b\}$, where $r_{h,x}$ denotes the server's estimate value given the shared randomness h and the received message x.

Accordingly, the discretized optimization problem is defined as:

$$
\begin{aligned}
\underset{s,r}{\text{minimize}} \quad & \frac{1}{m} \cdot \frac{1}{2^\ell} \cdot \sum_{h,q,x} s_{h,q,x} \cdot (q - r_{h,x})^2 \\
\text{subject to} \quad & \\
(\textit{Unbiasedness}) \quad & \frac{1}{2^\ell} \cdot \sum_{h,x} s_{h,q,x} \cdot r_{h,x} = q, && \forall q \\
(\textit{Probability}) \quad & \sum_{x} s_{h,q,x} = 1, && \forall h, q \\
& s_{h,q,x} \geqslant 0, && \forall h, q, x
\end{aligned}
$$

As mentioned, the solver's output does not directly yield an implementable algorithm, as it only associates probabilities to each $\langle h, q, x \rangle$ tuple. A natural option is to first stochastically quantize Z to a quantile. For example, when $Z = 1$ and using the $\mathcal{Q}_4$ described above, before applying the algorithm, we quantize it to $q^- = 0.4298$ with probability ≈ 0.786 or $q^+ = 3.097$ with probability ≈ 0.214.

This approach gives an algorithm whose pseudo-code is given in Algorithm 1. The resulting algorithm is near-optimal in the sense that as the number of quantiles and shared random bits tend to infinity, we converge to an optimal algorithm. In practice, the solver we use is only able to produce an output for finite m, ℓ values; this means that the algorithm would be optimal if coordinates are uniformly distributed over $\mathcal{Q}_m$, and not in $\mathcal{N}(0,1)$. Further, we observed that the solver has not fully converged for the highest ℓ values for which we were able to obtain an output. While the solver's result is still guaranteed to yield an unbiased algorithm, its error may be suboptimal. We explore these issues further in §4.

In words, in Algorithm 1 each client c uses shared randomness to compute a global random rotation $\mathcal{R}$ (note that all clients use the same rotation). Next, it computes the rotated vector $\mathcal{R}(x_c)$; for sufficiently large dimensions, the distribution of each entry in $\overline{Z}_c$ converges to $\mathcal{N}\left(0, \frac{\|x_c\|_2^2}{d}\right)$. The client then normalizes it, $\overline{Z}_c = \frac{\sqrt{d}}{\|x_c\|_2} \cdot \mathcal{R}(x_c)$, to have the coordinates roughly distributed $\mathcal{N}(0,1)$. Next, it stochastically quantizes the vector to $\mathcal{Q}_m$. Namely, for a given coordinate Z, let $q^-, q^+ \in \mathcal{Q}_m$ denote the largest quantile smaller or equal to Z, and the smallest quantile larger than q respectively. Then we denote by $\mathcal{Q}_m(Z)$ the stochastic quantization operation that returns q^+ with probability $\frac{Z - q^-}{q^+ - q^-}$ and q^- otherwise. The stochastic quantization of the vector applies coordinate-wise, i.e., $\mathcal{Q}_m(\overline{Z}_c) = (\mathcal{Q}_m(\overline{Z}_c[0]), \ldots, \mathcal{Q}_m(\overline{Z}_c[d-1]))$. The next step is to generate a client-specific shared randomness vector $\overline{H}_c$ in which each entry is drawn uniformly and independently from $\mathcal{H}_\ell$. Finally, the client follows the client algorithm produced by the solver. That is, for each coordinate Z, the client takes the mapped quantile $q = \mathcal{Q}_m(Z) \in \mathcal{Q}_m$, considers the set of probabilities $\{s_{h,q,x} \mid x \in \mathcal{X}_b\}$,

Algorithm 1

Client c:

1: Compute $\overline{Z}_c = \frac{\sqrt{d}}{\|x_c\|_2} \cdot \mathcal{R}(x_c)$.

2: Stochastically quantize $\widetilde{Z}_c = \mathcal{Q}_m(\overline{Z}_c)$

3: Sample $\overline{X}_c \sim \left\{x \text{ with prob. } s_{\overline{H}_c, \widetilde{Z}_c, x} \mid x \in \mathcal{X}_b\right\}$

4: Send $\left(\|x_c\|_2, \overline{X}_c\right)$ to server

Server:

1: $\forall c$: Compute $\widehat{\overline{Z}}_c = r_{\overline{H}_c, \overline{X}_c}$

2: Compute $\widehat{\overline{Z}}_{avg} = \frac{1}{n} \cdot \frac{1}{\sqrt{d}} \cdot \sum_{c=1}^{n} \|x_c\|_2 \cdot \widehat{\overline{Z}}_c$

3: Estimate $\widehat{x}_{avg} = \mathcal{R}^{-1}\left(\widehat{\overline{Z}}_{avg}\right)$

and samples a message accordingly. We denote applying this operation coordinate-wise by $\overline{X}_c \sim \left\{x \text{ with prob. } s_{\overline{H}_c, \widetilde{Z}_c, x} \mid x \in \mathcal{X}_b\right\}$. It then sends the resulting vector $\overline{X}_c$ to the server, together with the norm $\|x_c\|_2$. In turn, for each client c, the server estimates its rotated vector by looking up the shared randomness and message for each coordinate. That is, given $\overline{H}_c = (\overline{H}_c[0], \ldots, \overline{H}_c[d-1])$ and $\overline{X}_c = (\overline{X}_c[0], \ldots, \overline{X}_c[d-1])$ we denote $r_{\overline{H}_c, \overline{X}_c} = (r_{\overline{H}_c[0], \overline{X}_c[0]}, \ldots)$. The server then estimates $\mathcal{R}(x_c)$ as $\left(\|x_c\| / \sqrt{d} \cdot r_{\overline{H}_c, \overline{X}_c}\right)$ and averages across all clients before performing the inverse rotation. In the next section, we analyze the solver's output and show how to improve this method.

3.4 Interpolating the Solver's Solution

Based on our examination of solver outputs, we determined an alternative approach that does not stochastically quantize each coordinate to a quantile as above and empirically performs better.

We explain the process first considering an example. We consider the setting of $p = \frac{1}{512}$ ($T_p \approx 3.097$), $m = 512$ quantiles, $b = 2$ bits per coordinate, and $\ell = 2$ bits of shared randomness. One optimal solution for the server is given below:[5]

	$x=0$	$x=1$	$x=2$	$x=3$
$h=0$	-5.48	-1.23	**0.164**	1.68
$h=1$	-3.04	-0.831	**0.490**	2.18
$h=2$	-2.18	**-0.490**	0.831	3.04
$h=3$	-1.68	**-0.164**	1.23	5.48

Table 2: Optimal server values ($r_{h,x}$) for $x \in \mathcal{X}_2, H \in \mathcal{H}_2$ when $p = 1/512$ and $m = 512$, rounded to 3 significant digits. For example, when $Z = 0$, the server will estimate one of the values in bold based on the shared randomness and the message received from the client.

Given this table, by symmetry, if $Z = 0$ we can send $X = \begin{cases} 1 & \text{If } H \leqslant 1 \\ 2 & \text{Otherwise} \end{cases}$, which is formally written as $S_x(H, 0) = \begin{cases} 1 & \text{If } (x = 1 \wedge H \leqslant 1) \vee (x = 2 \wedge H > 1) \\ 0 & \text{Otherwise} \end{cases}$. Indeed, we have that $\mathbb{E}\left[\widehat{Z}\right] = \frac{1}{4}\sum_h r_{h,X} = 0$. Now, suppose that $Z > 0$ (the negative case is symmetric); the client can increase the server estimate's expected value (compared with the above choice of X) by moving probability mass to larger x values for some (or all) of the options for H. For any $Z \in (-T_p, T_p)$, there are infinitely many client alternatives that would yield an unbiased estimate. For example, if $Z = 0.1$, below are two client options (rounded to one significant digit):

$$S'_x(H, 0.1) \approx \begin{cases} 1 & \text{If } (x = 1 \wedge H \leqslant 2) \\ 0.6 & \text{If } (x = 2 \wedge H = 3) \\ 0.4 & \text{If } (x = 3 \wedge H = 3) \\ 0 & \text{Otherwise} \end{cases}, \quad S''_x(H, 0.1) \approx \begin{cases} 1 & \text{If } (x = 2 \wedge H \leqslant 1) \vee (x = 1 \wedge H = 3) \\ 0.3 & \text{If } (x = 1 \wedge H = 2) \\ 0.7 & \text{If } (x = 2 \wedge H = 2) \\ 0 & \text{Otherwise} \end{cases}$$

Note that while both S' and S'' produce unbiased estimates, their expected squared errors differ. Further, since $0.1 \notin \mathcal{Q}_m$, the solver's output does not directly indicate what is the optimal client's algorithm, even if the server table is fixed. Unlike Algorithm 1, which stochastically quantizes Z to either q^- or q^+, we studied the solver's output $\{s_{h,q,x}\}_{h,q,x}$ to interpolate the client to non-quantile values.

The approach we take corresponds to the following process. We move probability mass from the *leftmost, then uppermost* entry with mass to its right neighbor in the server table. So, for example,

[5] A crucial ingredient in getting a human-readable solution from the solver is that we, without loss of generality, force monotonicity in both h and x, i.e., $(x \geqslant x') \wedge (h \geqslant h') \implies r_{h,x} \geqslant r_{h',x'}$. Further, note that Table 2 is symmetric. We found tables were symmetric for small ℓ, m, and then forced symmetry in order to reduce model size for larger values. We use this symmetry in our interpolation.

Algorithm 2 QUIC-FL

Client c:

1: Compute $\overline{Z}_c = \frac{\sqrt{d}}{\|x_c\|_2} \cdot \mathcal{R}(x_c)$.
2: Compute $S(H_c, \overline{Z}_c)$ as in (9) given in Appendix C
3: Sample $\overline{X}_c \sim S(H_c, \overline{Z}_c)$
4: Send $\left(\|x_c\|_2, X_c\right)$ to server

Server:

1: $\forall c$: Compute $\widehat{\overline{Z}}_c = r_{\overline{H}_c, \overline{X}_c}$
2: Compute $\widehat{\overline{Z}}_{avg} = \frac{1}{n} \cdot \frac{1}{\sqrt{d}} \cdot \sum_{c=1}^{n} \|x_c\|_2 \cdot \widehat{\overline{Z}}_c$
3: Estimate $\widehat{x}_{avg} = \mathcal{R}^{-1}\left(\widehat{\overline{Z}}_{avg}\right)$

in Table 2, as Z increases from 0 we first move mass from the entry $x = 1, h = 2$ to the entry $x = 2, h = 2$. That is, the client, based on its private randomness, increases the probability of message $x = 2$ and decreases the probability of message $x = 1$ when $h = 2$. The amount of mass moved is always chosen to maintain unbiasedness. At some point, as Z increases, all of the probability mass will have moved, and then we start moving mass from $x = 1, h = 3$ similarly. (And subsequently, from $x = 2, h = 0$ and so on.) This process is visualized in Figure 1. Note that $S_x(h, z)$ values are piecewise linear as a function of z, and further, these values either go from 0 to 1, 1 to 0, or 0 to 1 and back again (all of which follow from our description). We can turn this description into formulae, and we defer this mathematical interpretation to Appendix C. The final algorithm, named QUIC-FL, is given by Algorithm 2 (based on the formula given in the appendix).

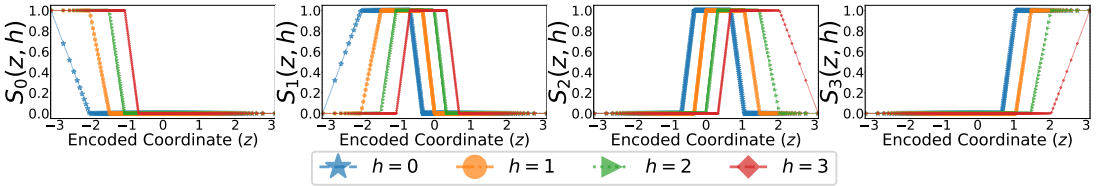


Figure 1: The solver's client algorithm (for $b = \ell = 2, m = 512, p = \frac{1}{512}$) *for the quantiles* $\{s_{h,q,x}\}_{h,q,x}$. Markers correspond to quantiles in $\mathcal{Q}_m$, and the lines illustrate our interpolation.

3.5 Hadamard

Similarly to previous rotation-based compression algorithms [3, 5, 7] we propose to use the Randomized Hadamard Transform (RHT) instead of uniform random rotations. Although RHT does not induce a uniform distribution on the sphere (and the coordinates are not exactly normally distributed), under mild assumptions, the resulting distribution is sufficiently close to the normal distribution [5]. Here, we are interested in how using RHT affects the guarantees of our algorithm. We analyze how using RHT affects our guarantees, starting by noting that our algorithm remains unbiased *for any input vector*. However, adversarial inputs may (1) increase the probability that a rotated coordinate falls outside $[-T_p, T_p]$ and (2) increase the $vNMSE$ as the coordinates' distribution deviates from the normal distribution. We show in Appendix D that QUIC-FL with RHT has similar guarantees as with random rotations, albeit somewhat weaker (constant factor increases in the fraction of accurately sent coordinates and $vNMSE$). We note that these guarantees are still stronger than those of DRIVE [5] and EDEN [7], which only prove RHT bounds for input vectors whose coordinates are sampled i.i.d. from a distribution with finite moments, and are not applicable to adversarial vectors. In practice, as shown in the evaluation, the actual performance is close to the theoretical results for uniform rotations; improving the bounds is left as future work. In our evaluation, we use QUIC-FL (Algorithm 2) with RHT-based vector rotation.

4 Evaluation

4.1 Theoretical Evaluation: $NMSE$ and Speed Measurements

Parameter Selection. We experiment with how the different parameters (number of quantiles m, the fraction of coordinates sent exactly p, the number of shared random bits ℓ, etc.) affect the performance of our algorithm. As shown in Figure 2, introducing shared randomness decreases the $vNMSE$ significantly compared with $\ell = 0$. Additionally, the benefit from adding each additional shared random bit diminishes, and the gain beyond $\ell = 4$ is negligible, especially for large b. Accordingly, we hereafter use $\ell = 6$ for $b = 1$, $\ell = 5$ for $b = 2$, and $\ell = 4$ for $b \in \{3, 4\}$. With respect to p, we determined $\frac{1}{512}$ as a good balance between the $vNMSE$ and bandwidth overhead.

Comparison to State of the Art DME techniques. Next, we compare the performance of QUIC-FL to the baseline algorithms in terms of $NMSE$, encoding speed, and decoding speed, using an NVIDIA 3080 RTX GPU machine with 32GB RAM and i7-10700K CPU @ 3.80GHz. Specifically, we compare with Hadamard [3], Kashin's representation [11, 12], QSGD [14], and EDEN [7]. We

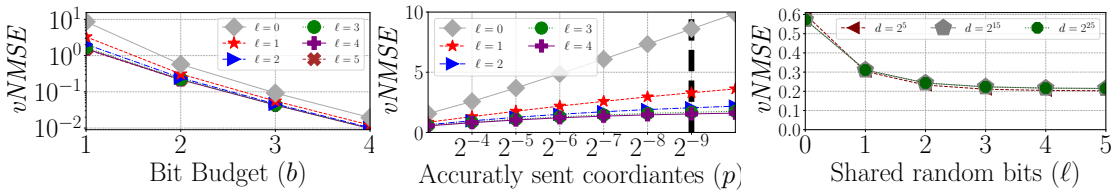


Figure 2: The $vNMSE$ of QUIC-FL as a function of the bit budget, fraction p, and shared random bits ℓ.

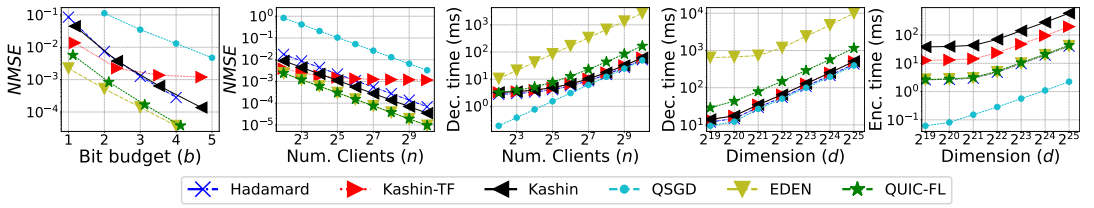


Figure 3: Comparison to alternative works with n clients that have the same $LogNormal(0, 1)$ input vector [5, 7]. The default values are $n = 256$ clients, $b = 4$ bit budget, and $d = 2^{20}$ dimensions.

evaluate two variants of Kashin's representation: (1) The TensorFlow (TF) implementation [21] that, by default, limits the decomposition to three iterations, and (2) the theoretical algorithm that requires $O(\log(nd))$ iterations. As shown in Figure 3, QUIC-FL has the second-lowest $NMSE$, slightly higher than EDEN's, which has a far slower decode time. Further, QUIC-FL is significantly more accurate than approaches with similar speeds. We observed that the default TF configuration of Kashin's representation suffers from a bias, and therefore its $NMSE$ does not decrease inversely proportional to n. In contrast, the theoretical algorithm is unbiased but has a markedly higher encoding time. We observed similar trends for different n, b, and d values. We consider the algorithms' bandwidth over all coordinates (e.g., with $b + \frac{64}{512}$ bits for QUIC-FL). Overall, the empirical measurements fall in line with the bounds in Table 1.

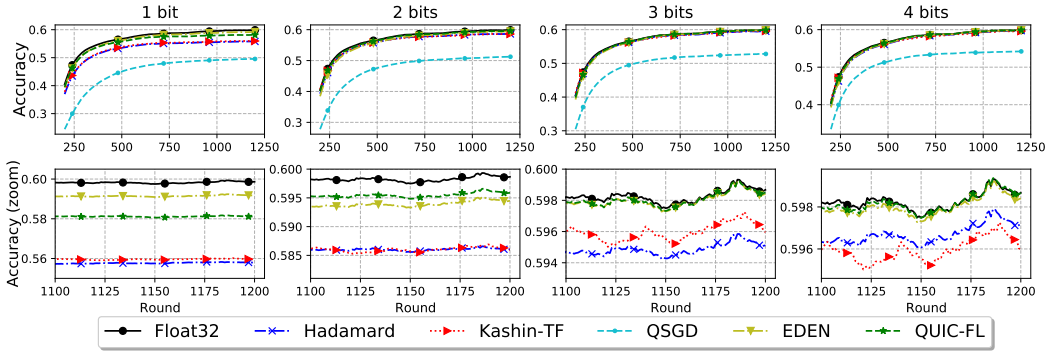


Figure 4: *FedAvg* over the Shakespeare next-word prediction task at various bit budgets (rows). We report training accuracy per round with a rolling mean window of 200 rounds. The second row zooms in on the last 100 rounds (QSGD is not included in the zoom since it performed poorly).

4.2 Federated Learning Experiments

Next-word prediction. We evaluate QUIC-FL over the Shakespeare next-word prediction task [22, 1] using an LSTM recurrent model. We run *FedAvg* [1] with the Adam server optimizer [23] and sample $n = 10$ clients per round. We use the setup from the federated learning benchmark of [24], restated for convenience in Appendix E. Figure 4 shows how QUIC-FL compares with other compression schemes at various bit budgets. As shown, QUIC-FL is competitive with EDEN and nearly matches the accuracy of the uncompressed baseline for $b \geqslant 3$.

Image classification. We evaluate QUIC-FL against other schemes with 10 persistent clients over uniformly distributed CIFAR-10 and CIFAR-100 datasets [25]. We also evaluate *Count-Sketch* [26] (CS), often used for federated compression schemes (e.g., [27]). For CIFAR-10 and CIFAR-100, we use ResNet-9 [28] and ResNet-18 [28], with learning rates of 0.1 and 0.05, respectively. For both datasets, the clients perform a single optimization step at each round. Our setting includes an SGD optimizer with a cross entropy loss criterion, a batch size of 128, and a bit budget $b = 1$.

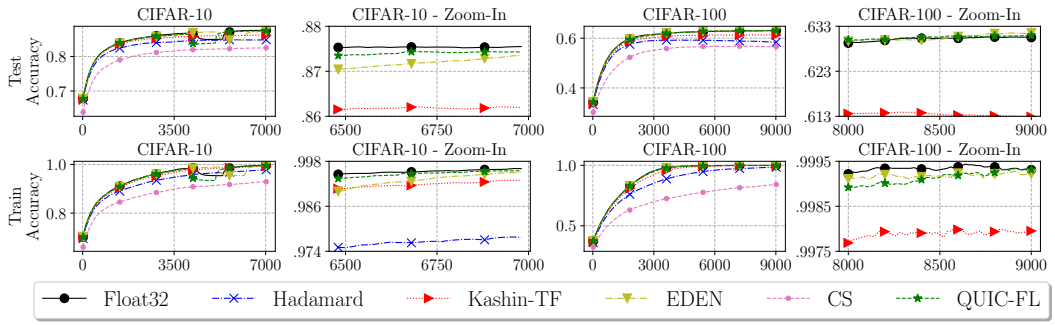


Figure 5: Train and test accuracy for CIFAR-10 and CIFAR-100 with 10 persistent clients (i.e., silos) and $b = 1$.

The results are shown in Figure 5, with a rolling mean average window of 500 rounds. As shown, QUIC-FL is competitive with EDEN and the Float32 baseline and is more accurate than other methods.

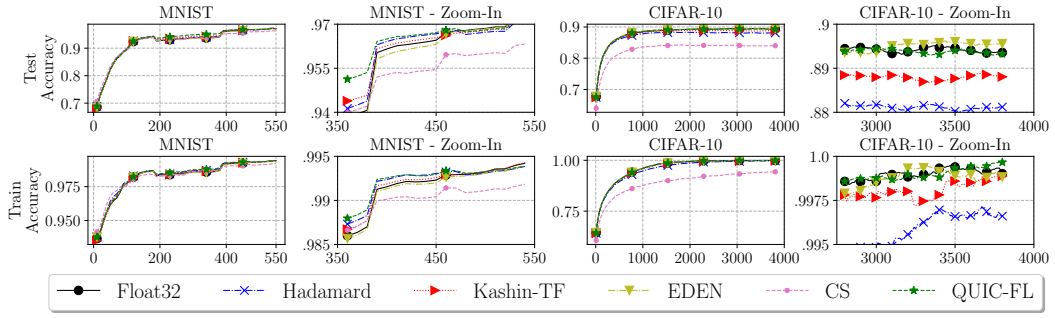


Figure 6: Cross-device federated learning of MNIST and CIFAR-10 with 50 clients ($b = 1$).

Next, we consider a highly heterogeneous cross-device setup with 50 clients over MNIST and CIFAR-10 datasets [25, 29, 30]. For MNIST, each client stores only a single class of the dataset and trains LeNet-5 [29] with a learning rate of 0.05. For CIFAR-10, all clients have the same data distribution, and each trains ResNet-9 [28] with a learning rate of 0.1. At each training round, 10 clients are randomly selected and perform training over 5 local steps. We use an SGD optimizer with a cross entropy loss criterion, a batch size of 128, and a bit budget $b = 1$.

Figure 6 shows the results with a rolling mean window of 200 rounds. Again, QUIC-FL is competitive with EDEN and the uncompressed baseline. Kashin-TF is less accurate followed by Hadamard.

Additional Evaluation Due to lack of space, we defer additional evaluation results to Appendix F.

5 Discussion

In this work, we presented QUIC-FL, a quick unbiased compression algorithm for federated learning. Both theoretically and empirically, QUIC-FL achieves an $NMSE$ that is comparable with the most accurate DME techniques, while allowing an asymptotically faster decode time.

We point out a few challenging directions for future work. QUIC-FL optimizes the worst-case error, and while it is compatible with orthogonal directions such as sparsification [4, 7, 31, 32], it is unclear how it would leverage potential correlations between coordinates [33] or client vectors [6]. Another direction for future research is understanding how to incorporate non-linear aggregation functions, such as approximate geometric median, that have shown to improve the training robustness [34].

Acknowledgments and Disclosure of Funding

Gil Einziger was funded in part by the Data Science Research Center at Ben-Gurion University. Michael Mitzenmacher was supported in part by NSF grants CCF-2101140, CNS-2107078, and DMS-2023528, and by a gift to the Center for Research on Computation and Society at Harvard University.

References

[1] H. Brendan McMahan, Eider Moore, Daniel Ramage, Seth Hampson, and Blaise Agüera y Arcas. Communication-Efficient Learning of Deep Networks from Decentralized Data. In *Artificial Intelligence and Statistics*, pages 1273–1282, 2017.

[2] Peter Kairouz, H. Brendan McMahan, Brendan Avent, Aurélien Bellet, Mehdi Bennis, Arjun Nitin Bhagoji, Keith Bonawitz, Zachary Charles, Graham Cormode, Rachel Cummings, Rafael G. L. D'Oliveira, Salim El Rouayheb, David Evans, Josh Gardner, Zachary Garrett, Adrià Gascón, Badih Ghazi, Phillip B. Gibbons, Marco Gruteser, Zaid Harchaoui, Chaoyang He, Lie He, Zhouyuan Huo, Ben Hutchinson, Justin Hsu, Martin Jaggi, Tara Javidi, Gauri Joshi, Mikhail Khodak, Jakub Konečný, Aleksandra Korolova, Farinaz Koushanfar, Sanmi Koyejo, Tancrède Lepoint, Yang Liu, Prateek Mittal, Mehryar Mohri, Richard Nock, Ayfer Özgür, Rasmus Pagh, Mariana Raykova, Hang Qi, Daniel Ramage, Ramesh Raskar, Dawn Song, Weikang Song, Sebastian U. Stich, Ziteng Sun, Ananda Theertha Suresh, Florian Tramèr, Praneeth Vepakomma, Jianyu Wang, Li Xiong, Zheng Xu, Qiang Yang, Felix X. Yu, Han Yu, and Sen Zhao. Advances and Open Problems in Federated Learning, 2019.

[3] Ananda Theertha Suresh, X Yu Felix, Sanjiv Kumar, and H Brendan McMahan. Distributed Mean Estimation With Limited Communication. In *International Conference on Machine Learning*, pages 3329–3337. PMLR, 2017.

[4] Jakub Konečnỳ and Peter Richtárik. Randomized Distributed Mean Estimation: Accuracy vs. Communication. *Frontiers in Applied Mathematics and Statistics*, 4:62, 2018.

[5] Shay Vargaftik, Ran Ben Basat, Amit Portnoy, Gal Mendelson, Yaniv Ben-Itzhak, and Michael Mitzenmacher. DRIVE: One-bit Distributed Mean Estimation. In *NeurIPS*, 2021.

[6] Peter Davies, Vijaykrishna Gurunanthan, Niusha Moshrefi, Saleh Ashkboos, and Dan Alistarh. New Bounds For Distributed Mean Estimation and Variance Reduction. In *International Conference on Learning Representations*, 2021.

[7] Shay Vargaftik, Ran Ben Basat, Amit Portnoy, Gal Mendelson, Yaniv Ben-Itzhak, and Michael Mitzenmacher. Communication-efficient federated learning via robust distributed mean estimation. *arXiv preprint arXiv:2108.08842*, 2021.

[8] Youhui Bai, Cheng Li, Quan Zhou, Jun Yi, Ping Gong, Feng Yan, Ruichuan Chen, and Yinlong Xu. Gradient compression supercharged high-performance data parallel dnn training. In *The 28th ACM Symposium on Operating Systems Principles (SOSP 2021)*, 2021.

[9] Yuchen Zhong, Cong Xie, Shuai Zheng, and Haibin Lin. Compressed communication for distributed training: Adaptive methods and system. *arXiv preprint arXiv:2105.07829*, 2021.

[10] Yurii Lyubarskii and Roman Vershynin. Uncertainty Principles and Vector Quantization. *IEEE Transactions on Information Theory*, 56(7):3491–3501, 2010.

[11] Sebastian Caldas, Jakub Konečný, H Brendan McMahan, and Ameet Talwalkar. Expanding the Reach of Federated Learning by Reducing Client Resource Requirements. *arXiv preprint arXiv:1812.07210*, 2018.

[12] Mher Safaryan, Egor Shulgin, and Peter Richtárik. Uncertainty principle for communication compression in distributed and federated learning and the search for an optimal compressor. *Information and Inference: A Journal of the IMA*, 2020.

[13] Ran Ben Basat, Michael Mitzenmacher, and Shay Vargaftik. How to send a real number using a single bit (and some shared randomness). In *48th International Colloquium on Automata, Languages, and Programming (ICALP 2021)*, 2021.

[14] Dan Alistarh, Demjan Grubic, Jerry Li, Ryota Tomioka, and Milan Vojnovic. QSGD: Communication-Efficient SGD via Gradient Quantization and Encoding. *Advances in Neural Information Processing Systems*, 30:1709–1720, 2017.

[15] Adam Paszke, Sam Gross, Francisco Massa, Adam Lerer, James Bradbury, Gregory Chanan, Trevor Killeen, Zeming Lin, Natalia Gimelshein, Luca Antiga, Alban Desmaison, Andreas Kopf, Edward Yang, Zachary DeVito, Martin Raison, Alykhan Tejani, Sasank Chilamkurthy, Benoit Steiner, Lu Fang, Junjie Bai, and Soumith Chintala. PyTorch: An Imperative Style, High-Performance Deep Learning Library. In H. Wallach, H. Larochelle, A. Beygelzimer, F. d'Alché-Buc, E. Fox, and R. Garnett, editors, *Advances in Neural Information Processing Systems 32*, pages 8026–8037. Curran Associates, Inc., 2019.

[16] Martín Abadi, Ashish Agarwal, Paul Barham, Eugene Brevdo, Zhifeng Chen, Craig Citro, Greg S. Corrado, Andy Davis, Jeffrey Dean, Matthieu Devin, Sanjay Ghemawat, Ian Goodfellow, Andrew Harp, Geoffrey Irving, Michael Isard, Yangqing Jia, Rafal Jozefowicz, Lukasz Kaiser, Manjunath Kudlur, Josh Levenberg, Dandelion Mané, Rajat Monga, Sherry Moore, Derek Murray, Chris Olah, Mike Schuster, Jonathon Shlens, Benoit Steiner, Ilya Sutskever, Kunal Talwar, Paul Tucker, Vincent Vanhoucke, Vijay Vasudevan, Fernanda Viégas, Oriol Vinyals, Pete Warden, Martin Wattenberg, Martin Wicke, Yuan Yu, and Xiaoqiang Zheng. TensorFlow: Large-Scale Machine Learning on Heterogeneous Systems, 2015. Software available from tensorflow.org.

[17] Logan Beal, Daniel Hill, R Martin, and John Hedengren. Gekko optimization suite. *Processes*, 6(8):106, 2018.

[18] John D. Hedengren, Reza Asgharzadeh Shishavan, Kody M. Powell, and Thomas F. Edgar. Nonlinear modeling, estimation and predictive control in APMonitor. *Computers & Chemical Engineering*, 70:133 – 148, 2014. Manfred Morari Special Issue.

[19] Interior Point Optimizer (IPOPT) Solver. `https://coin-or.github.io/Ipopt/`.

[20] Advanced Process OPTimizer (APOPT) Solver. `https://github.com/APMonitor/apopt`.

[21] The TensorFlow Authors. TensorFlow Federated: Compression via Kashin's representation from Hadamard transform. `https://github.com/tensorflow/model-optimization/blob/9193d70f6e7c9f78f7c63336bd68620c4bc6c2ca/tensorflow_model_optimization/python/core/internal/tensor_encoding/stages/research/kashin.py#L92`. accessed 19-May-22.

[22] William Shakespeare. The Complete Works of William Shakespeare. `https://www.gutenberg.org/ebooks/100`.

[23] Diederik P. Kingma and Jimmy Ba. Adam: A Method for Stochastic Optimization. In *International Conference on Learning Representations*, 2015.

[24] Sashank J. Reddi, Zachary Charles, Manzil Zaheer, Zachary Garrett, Keith Rush, Jakub Konečný, Sanjiv Kumar, and Hugh Brendan McMahan. Adaptive Federated Optimization. In *International Conference on Learning Representations*, 2021.

[25] Alex Krizhevsky, Geoffrey Hinton, et al. Learning Multiple Layers of Features From Tiny Images. *Master's thesis, University of Toronto*, 2009.

[26] Moses Charikar, Kevin Chen, and Martin Farach-Colton. Finding frequent items in data streams. In *International Colloquium on Automata, Languages, and Programming*, pages 693–703. Springer, 2002.

[27] Nikita Ivkin, Daniel Rothchild, Enayat Ullah, Vladimir Braverman, Ion Stoica, and Raman Arora. Communication-Efficient Distributed SGD With Sketching. *Advances in neural information processing systems*, 2019.

[28] Kaiming He, Xiangyu Zhang, Shaoqing Ren, and Jian Sun. Deep Residual Learning for Image Recognition. In *Proceedings of the IEEE conference on computer vision and pattern recognition*, pages 770–778, 2016.

[29] Yann LeCun, Léon Bottou, Yoshua Bengio, and Patrick Haffner. Gradient-Based Learning Applied to Document Recognition. *Proceedings of the IEEE*, 86(11):2278–2324, 1998.

[30] Yann LeCun, Corinna Cortes, and CJ Burges. Mnist handwritten digit database. *ATT Labs [Online]. Available: http://yann.lecun.com/exdb/mnist*, 2, 2010.

[31] Jakub Konečný, H. Brendan McMahan, Felix X. Yu, Peter Richtárik, Ananda Theertha Suresh, and Dave Bacon. Federated Learning: Strategies for Improving Communication Efficiency, 2017.

[32] Jiawei Fei, Chen-Yu Ho, Atal N Sahu, Marco Canini, and Amedeo Sapio. Efficient Sparse Collective Communication and its Application to Accelerate Distributed Deep Learning. In *Proceedings of the 2021 ACM SIGCOMM 2021 Conference*, pages 676–691, 2021.

[33] Nicole Mitchell, Johannes Ballé, Zachary Charles, and Jakub Konečnỳ. Optimizing the communication-accuracy trade-off in federated learning with rate-distortion theory. *arXiv preprint arXiv:2201.02664*, 2022.

[34] Krishna Pillutla, Sham M Kakade, and Zaid Harchaoui. Robust aggregation for federated learning. *IEEE Transactions on Signal Processing*, 70:1142–1154, 2022.

[35] Aleksandr Beznosikov, Samuel Horváth, Peter Richtárik, and Mher Safaryan. On Biased Compression For Distributed Learning. *arXiv preprint arXiv:2002.12410*, 2020.

[36] Frank Seide, Hao Fu, Jasha Droppo, Gang Li, and Dong Yu. 1-Bit Stochastic Gradient Descent and Its Application to Data-Parallel Distributed Training of Speech DNNs. In *Fifteenth Annual Conference of the International Speech Communication Association*, 2014.

[37] Dan-Adrian Alistarh, Torsten Hoefler, Mikael Johansson, Nikola H Konstantinov, Sarit Khirirat, and Cedric Renggli. The Convergence of Sparsified Gradient Methods. *Advances in Neural Information Processing Systems*, 31, 2018.

[38] Peter Richtárik, Igor Sokolov, and Ilyas Fatkhullin. EF21: A New, Simpler, Theoretically Better, and Practically Faster Error Feedback. In *Advances in Neural Information Processing Systems*, 2021.

[39] Sebastian U Stich, Jean-Baptiste Cordonnier, and Martin Jaggi. Sparsified SGD with Memory. In S. Bengio, H. Wallach, H. Larochelle, K. Grauman, N. Cesa-Bianchi, and R. Garnett, editors, *Advances in Neural Information Processing Systems*, volume 31. Curran Associates, Inc., 2018.

[40] Konstantin Mishchenko, Eduard Gorbunov, Martin Takáč, and Peter Richtárik. Distributed Learning With Compressed Gradient Differences. *arXiv preprint arXiv:1901.09269*, 2019.

[41] Eduard Gorbunov, Konstantin P. Burlachenko, Zhize Li, and Peter Richtarik. MARINA: Faster Non-Convex Distributed Learning with Compression. In *Proceedings of the 38th International Conference on Machine Learning*, volume 139 of *Proceedings of Machine Learning Research*, pages 3788–3798. PMLR, 18–24 Jul 2021.

[42] Amedeo Sapio, Marco Canini, Chen-Yu Ho, Jacob Nelson, Panos Kalnis, Changhoon Kim, Arvind Krishnamurthy, Masoud Moshref, Dan Ports, and Peter Richtarik. Scaling Distributed Machine Learning with In-Network Aggregation. In *18th USENIX Symposium on Networked Systems Design and Implementation (NSDI 21)*, pages 785–808, 2021.

[43] ChonLam Lao, Yanfang Le, Kshiteej Mahajan, Yixi Chen, Wenfei Wu, Aditya Akella, and Michael Swift. ATP: In-network Aggregation for Multi-tenant Learning. In *18th USENIX Symposium on Networked Systems Design and Implementation (NSDI 21)*, pages 741–761, 2021.

[44] Raz Segal, Chen Avin, and Gabriel Scalosub. SOAR: Minimizing Network Utilization with Bounded In-network Computing. In *Proceedings of the 17th International Conference on emerging Networking EXperiments and Technologies*, pages 16–29, 2021.

[45] Sebastian U Stich, Jean-Baptiste Cordonnier, and Martin Jaggi. Sparsified sgd with memory. *Advances in Neural Information Processing Systems*, 31, 2018.

[46] Alham Fikri Aji and Kenneth Heafield. Sparse Communication for Distributed Gradient Descent. In *Proceedings of the 2017 Conference on Empirical Methods in Natural Language Processing*, pages 440–445, 2017.

[47] Yujun Lin, Song Han, Huizi Mao, Yu Wang, and Bill Dally. Deep Gradient Compression: Reducing the Communication Bandwidth for Distributed Training. In *International Conference on Learning Representations*, 2018.

[48] Ananda Theertha Suresh, Ziteng Sun, Jae Hun Ro, and Felix Yu. Correlated quantization for distributed mean estimation and optimization. In *International Conference on Machine Learning*, 2022.

[49] Ran Ben Basat, Gil Einziger, Michael Mitzenmacher, and Shay Vargaftik. Faster and more accurate measurement through additive-error counters. In *IEEE INFOCOM 2020-IEEE Conference on Computer Communications*, pages 1251–1260. IEEE, 2020.

[50] Ran Ben Basat, Gil Einziger, Michael Mitzenmacher, and Shay Vargaftik. Salsa: Self-adjusting lean streaming analytics. In *2021 IEEE 37th International Conference on Data Engineering (ICDE)*, pages 864–875. IEEE, 2021.

[51] Ran Ben Basat, Sivaramakrishnan Ramanathan, Yuliang Li, Gianni Antichi, Minian Yu, and Michael Mitzenmacher. Pint: Probabilistic in-band network telemetry. In *Proceedings of the Annual conference of the ACM Special Interest Group on Data Communication on the*

applications, technologies, architectures, and protocols for computer communication, pages 662–680, 2020.

[52] Ran Ben Basat, Gil Einziger, Isaac Keslassy, Ariel Orda, Shay Vargaftik, and Erez Waisbard. Memento: Making sliding windows efficient for heavy hitters. *IEEE/ACM Transactions on Networking*, 2022.

[53] Mehrdad Khani, Manya Ghobadi, Mohammad Alizadeh, Ziyi Zhu, Madeleine Glick, Keren Bergman, Amin Vahdat, Benjamin Klenk, and Eiman Ebrahimi. Sip-ml: high-bandwidth optical network interconnects for machine learning training. In *Proceedings of the 2021 ACM SIGCOMM 2021 Conference*, pages 657–675, 2021.

[54] Ashish Goel, Michael Kapralov, and Sanjeev Khanna. Perfect Matchings in O(nlogn) Time in Regular Bipartite Graphs. *SIAM Journal on Computing*, 2013.

[55] Xin Sunny Huang, Xiaoye Steven Sun, and TS Ng. Sunflow: Efficient optical circuit scheduling for coflows. In *ACM CoNEXT*, 2016.

[56] He Liu, Matthew K Mukerjee, Conglong Li, et al. Scheduling techniques for hybrid circuit/packet networks. In *ACM CoNEXT*, 2015.

[57] Shay Vargaftik, Katherine Barabash, Yaniv Ben-Itzhak, Ofer Biran, Isaac Keslassy, Dean Lorenz, and Ariel Orda. Composite-path switching. In *Proceedings of the 12th International on Conference on emerging Networking Experiments and Technologies*, pages 329–343, 2016.

[58] Ariel Livshits and Shay Vargaftik. Lumos: A fast and efficient optical circuit switch scheduling technique. *IEEE Communications Letters*, 22(10):2028–2031, 2018.

[59] Shaileshh Bojja Venkatakrishnan, Mohammad Alizadeh, and Pramod Viswanath. Costly circuits, submodular schedules and approximate carathéodory theorems. *Queueing Systems*, 2018.

[60] Shay Vargaftik, Cosmin Caba, Liran Schour, and Yaniv Ben-Itzhak. C-share: Optical circuits sharing for software-defined data-centers. *ACM SIGCOMM Computer Communication Review*, 50(1):2–9, 2020.

[61] Jianyu Wang, Zachary Charles, Zheng Xu, Gauri Joshi, H Brendan McMahan, Maruan Al-Shedivat, Galen Andrew, Salman Avestimehr, Katharine Daly, Deepesh Data, et al. A Field Guide to Federated Optimization. *arXiv preprint arXiv:2107.06917*, 2021.

[62] Mervin E Muller. A Note on a Method for Generating Points Uniformly on N-Dimensional Spheres. *Communications of the ACM*, 2(4):19–20, 1959.

[63] Felix Xinnan X Yu, Ananda Theertha Suresh, Krzysztof M Choromanski, Daniel N Holtmann-Rice, and Sanjiv Kumar. Orthogonal Random Features. *Advances in neural information processing systems*, 29:1975–1983, 2016.

[64] Alexandr Andoni, Piotr Indyk, Thijs Laarhoven, Ilya Razenshteyn, and Ludwig Schmidt. Practical and Optimal LSH for Angular Distance. In *Proceedings of the 28th International Conference on Neural Information Processing Systems*, pages 1225–1233, 2015.

[65] Vidmantas Kastytis Bentkus and Dainius Dzindzalieta. A tight gaussian bound for weighted sums of rademacher random variables. *Bernoulli*, 21(2):1231–1237, 2015.

[66] S. Hochreiter and J. Schmidhuber. Long Short-Term Memory. *Neural Computation*, 9:1735–1780, 1997.

A Alternative Compression Methods

This paper focused on the Distributed Mean Estimation (DME) problem where clients send lossily compressed gradients to a centralized server for averaging. While this problem is worthy of study on its own merits, we are particularly interested in applications to federated learning, where there are many variations and practical considerations, which have led to many alternative compression methods to be considered. For example, when the encoding and decoding time is less important, different approaches suggest to use entropy encodings such as Huffman or arithmetic encoding to improve the accuracy (e.g., [3, 7, 14]). Intuitively, such encodings allow us to losslessly compress the lossily compressed vector to reduce its representation size, thereby allowing less aggressive quantization. However, we are unaware of available GPU-friendly entropy encoding implementation and thus such methods incur a significant time overhead.

Critically, for the basic DME problem, the assumption is that this is a one-shot process where the goal is to optimize the accuracy without relying on client-side memory. This model naturally fits cross-device federated learning, where different clients are sampled in each round. We focused on unbiased compression, which is standard in prior works [3, 4, 5, 6, 33]. However, if the compression error is low enough, and under some assumptions, SGD can be proven to converge even with biased compression [35].

In other settings, such as distributed learning or cross-silo federated learning, we may assume that clients are persistent and have a memory that keeps states between rounds. A prominent option to leverage such a state is to use Error Feedback (EF). In EF, clients can track the compression error and add it to the gradient computed in the consecutive round. This scheme is often shown to recover the model's convergence rate and resulting accuracy [36, 37, 38] and enables biased compressors such as Top-k [39].

An orthogonal proposal that works with persistent clients, which is also applicable with QUIC-FL, is to encode the difference between the current gradient and the previous one, instead of directly compressing the gradient [40, 41]. Broadly speaking, this allows a compression error that is proportional to the size of the difference and not the gradient, and can decrease the error if consecutive gradients are similar to each other.

When running distributed learning in cluster settings, recent works show how in-network aggregation can accelerate the learning process [42, 43, 44]. Intuitively, as switches are designed to move data at high speeds and recent advances in switch programmability enable it to easily perform simple aggregation operations like summation while processing the data.

Another line of work focuses on sparsifying the gradients before compressing them [32, 45, 46]. Intuitively, in some learning settings, many of the coordinates are small. and we can improve the accuracy to bandwidth tradeoff by removing all small coordinates prior to compression. Another form of sparsification is random sampling, which allows us to avoid sending the coordinate indices [7, 31]. We note that combining such approaches with QUIC-FL is straightforward, as we can compress the non-zero entries of the sparsified vectors.

Combining several techniques, including warm-up training, gradient clipping, momentum factor masking, momentum correction, and deep gradient compression [47], reports savings of two orders of magnitude in the bandwidth required for distributed learning. Another promising orthogonal approach is to leverage shared randomness to get the clients' compression to yield errors in opposite directions, thus making them cancel out and lowering the overall NMSE [48].

Compression is also fundamental in network telemetry [49, 50], where it allows devices to communicate fewer bits while ensuring accurate network-wide view at the controller [51, 52].

Another, often orthogonal, approach to accelerate DNN training and improve its efficiency is to use emerging high-bandwidth and energy-efficient technologies such as optical switching [53] with matching low-latency scheduling techniques (e.g., [54, 55, 56, 57, 58, 59, 60]).

We refer the reader to [2, 31, 61] for an extensive review of the current state of the art and challenges.

B QUIC-FL's $vNMSE$ Proof

Theorem 1. *For Algorithms 1 and 2 and a uniform rotation, it holds that, for $Z \sim \mathcal{N}(0,1)$:*

$$vNMSE \leqslant \mathbb{E}\left[\left(Z-\widehat{Z}\right)^2\right] + O\left(\sqrt{\frac{\log d}{d}}\right) .$$

Proof. The proof follows similar lines to that of [5, 7]. However, here the $vNMSE$ expression is different and is somewhat simpler as it takes advantage of our *unbiased* quantization technique.

A rotation preserves a vector's euclidean norm. Thus, according to Algorithms 1 and 2 it holds that

$$\begin{aligned}\left\|x-\widehat{x}\right\|_2^2 = \left\|\mathcal{R}\left(x-\widehat{x}\right)\right\|_2^2 = \left\|\mathcal{R}\left(x\right)-\mathcal{R}\left(\widehat{x}\right)\right\|_2^2 = \\ \left\|\frac{\left\|x\right\|_2}{\sqrt{d}}\cdot\overline{Z}-\frac{\left\|x\right\|_2}{\sqrt{d}}\cdot\widehat{\overline{Z}}\right\|_2^2 = \frac{\left\|x\right\|_2^2}{d}\cdot\left\|\overline{Z}-\widehat{\overline{Z}}\right\|_2^2 .\end{aligned} \tag{1}$$

Taking expectation and dividing by $\left\|x\right\|_2^2$ yields

$$\begin{aligned}vNMSE \triangleq \mathbb{E}\left[\frac{\left\|x-\widehat{x}\right\|_2^2}{\left\|x\right\|_2^2}\right] =& \frac{1}{d}\cdot\mathbb{E}\left[\left\|\overline{Z}-\widehat{\overline{Z}}\right\|_2^2\right] \\ =& \frac{1}{d}\cdot\mathbb{E}\left[\sum_{i=1}^{d}\left(\overline{Z}[i]-\widehat{\overline{Z}}[i]\right)^2\right] = \frac{1}{d}\cdot\sum_{i=1}^{d}\mathbb{E}\left[\left(\overline{Z}[i]-\widehat{\overline{Z}}[i]\right)^2\right] .\end{aligned} \tag{2}$$

Let $\tilde{Z}=(\tilde{Z}_1,\ldots,\tilde{Z}_d)$ be a vector of independent $\mathcal{N}(0,1)$ random variables. Then, the distribution of each coordinate $\overline{Z}[i]$ is given by $\tilde{Z}[i] \sim \sqrt{d}\cdot\frac{\tilde{Z}[i]}{\left\|\tilde{Z}\right\|_2}$ (e.g., see [62, 5]).

This means that all coordinates of $\overline{Z}$ and thus all coordinates of $\widehat{\overline{Z}}$ follow the same distribution. Thus, without loss of generality, we obtain

$$vNMSE \triangleq \mathbb{E}\left[\frac{\left\|x-\widehat{x}\right\|_2^2}{\left\|x\right\|_2^2}\right] = \mathbb{E}\left[\left(\overline{Z}[0]-\widehat{\overline{Z}}[0]\right)^2\right] = \mathbb{E}\left[\left(\frac{\sqrt{d}}{\left\|\tilde{Z}\right\|_2}\cdot\tilde{Z}[0]-\widehat{\overline{Z}}[0]\right)^2\right] . \tag{3}$$

For some $0<\alpha<\frac{1}{2}$, denote the event

$$A = \left\{d\cdot(1-\alpha) \leqslant \left\|\tilde{Z}\right\|_2^2 \leqslant d\cdot(1+\alpha)\right\} .$$

Let A^c be the complementary event of A. By Lemma D.2 in [7] it holds that $\mathbb{P}(A^c) \leqslant 2\cdot e^{-\frac{\alpha^2}{8}\cdot d}$. Also, by the law of total expectation

$$\begin{aligned}&\mathbb{E}\left[\left(\frac{\sqrt{d}}{\left\|\tilde{Z}\right\|_2}\cdot\tilde{Z}[0]-\widehat{\overline{Z}}[0]\right)^2\right] \leqslant \\ &\mathbb{E}\left[\left(\frac{\sqrt{d}}{\left\|\tilde{Z}\right\|_2}\cdot\tilde{Z}[0]-\widehat{\overline{Z}}[0]\right)^2\middle|A\right]\cdot\mathbb{P}(A)+\mathbb{E}\left[\left(\frac{\sqrt{d}}{\left\|\tilde{Z}\right\|_2}\cdot\tilde{Z}[0]-\widehat{\overline{Z}}[0]\right)^2\middle|A^c\right]\cdot\mathbb{P}(A^c) \leqslant \\ &\mathbb{E}\left[\left(\frac{\sqrt{d}}{\left\|\tilde{Z}\right\|_2}\cdot\tilde{Z}[0]-\widehat{\overline{Z}}[0]\right)^2\middle|A\right]\cdot\mathbb{P}(A)+M\cdot\mathbb{P}(A^c) ,\end{aligned} \tag{4}$$

where $M = (vNMSE_{max})^2$ and $vNMSE_{max}$ is the maximal value at the server's reconstruction table (i.e., $\max(r)$) which is a constant that is *independent* of the vector's dimension. Next,

$$\mathbb{E}\left[\left(\frac{\sqrt{d}}{\left\|\tilde{Z}\right\|_2}\cdot\tilde{Z}[0]-\widehat{\tilde{Z}}[0]\right)^2\Big|A\right]=\mathbb{E}\left[\left(\left(\tilde{Z}[0]-\widehat{\tilde{Z}}[0]\right)+\left(\frac{\sqrt{d}}{\left\|\tilde{Z}\right\|_2}-1\right)\cdot\tilde{Z}[0]\right)^2\Big|A\right]=$$
$$\mathbb{E}\left[\left(\tilde{Z}[0]-\widehat{\tilde{Z}}[0]\right)^2\Big|A\right]+2\cdot\mathbb{E}\left[\left(\tilde{Z}[0]-\widehat{\tilde{Z}}[0]\right)\cdot\left(\frac{\sqrt{d}}{\left\|\tilde{Z}\right\|_2}-1\right)\cdot\tilde{Z}[0]\Big|A\right]+$$
$$\mathbb{E}\left[\left(\left(\frac{\sqrt{d}}{\left\|\tilde{Z}\right\|_2}-1\right)\cdot\tilde{Z}[0]\right)^2\Big|A\right] \tag{5}$$

Also,

$$\begin{aligned}&\mathbb{E}\left[\left(\tilde{Z}[0]-\widehat{\tilde{Z}}[0]\right)\cdot\left(\frac{\sqrt{d}}{\left\|\tilde{Z}\right\|_2}-1\right)\cdot\tilde{Z}[0]\Big|A\right]\cdot\mathbb{P}(A)\leqslant\\&\left(\frac{1}{\sqrt{1-\alpha}}-1\right)\cdot\left|\mathbb{E}\left[\left(\tilde{Z}[0]-\widehat{\tilde{Z}}[0]\right)\cdot\tilde{Z}[0]|A\right]\cdot\mathbb{P}(A)\right|\leqslant\\&\left(\frac{1}{\sqrt{1-\alpha}}-1\right)\cdot\left|\mathbb{E}\left[\left(\tilde{Z}[0]\right)^2-\widehat{\tilde{Z}}[0]\cdot\tilde{Z}[0]\Big|A\right]\cdot\mathbb{P}(A)\right|\leqslant\\&\left(\frac{1}{\sqrt{1-\alpha}}-1\right)\cdot 1+\left(\frac{1}{\sqrt{1-\alpha}}-1\right)\cdot\frac{1}{\sqrt{1-\alpha}}=\frac{\alpha}{1-\alpha}\leqslant 2\alpha\,.\end{aligned} \tag{6}$$

Here, we used that $\mathbb{E}\left[\left(\tilde{Z}[0]\right)^2|A\right]\cdot\mathbb{P}(A)\leqslant\mathbb{E}\left[\left(\tilde{Z}[0]\right)^2\right]=1$ and that $\mathbb{E}\left[\widehat{\tilde{Z}}[0]\cdot\tilde{Z}[0]|A\right]\cdot\mathbb{P}(A)=\mathbb{E}\left[\mathbb{E}\left[\widehat{\tilde{Z}}[0]\cdot\tilde{Z}[0]|A,\tilde{Z}\right]\right]\cdot\mathbb{P}(A)=\mathbb{E}\left[\frac{\sqrt{d}}{\left\|\tilde{Z}\right\|_2}\cdot\left(\tilde{Z}[0]\right)^2|A\right]\cdot\mathbb{P}(A)\leqslant\frac{1}{\sqrt{1-\alpha}}\cdot\mathbb{E}\left[\left(\tilde{Z}[0]\right)^2\right]=\frac{1}{\sqrt{1-\alpha}}$.
Next, we similarly obtain

$$\mathbb{E}\left[\left(\left(\frac{\sqrt{d}}{\left\|\tilde{Z}\right\|_2}-1\right)\cdot\tilde{Z}[0]\right)^2\Big|\,A\right]\cdot\mathbb{P}(A)\leqslant\quad\left(\frac{1}{\sqrt{1-\alpha}}-1\right)+\left(1-\frac{1}{\sqrt{1+\alpha}}\right)\leqslant 2\alpha. \tag{7}$$

Thus,

$$vNMSE\leqslant\mathbb{E}\left[\left(\tilde{Z}[0]-\widehat{\tilde{Z}}[0]\right)^2\right]+4\alpha+2\cdot e^{-\frac{\alpha^2}{8}\cdot d}\cdot M\,. \tag{8}$$

Setting $\alpha=\sqrt{\frac{8\log d}{d}}$ yields $vNMSE\leqslant\mathbb{E}\left[\left(\tilde{Z}[0]-\widehat{\tilde{Z}}[0]\right)^2\right]+O\left(\sqrt{\frac{\log d}{d}}\right)$.

Finally, since $\widetilde{Z}[0]\sim\mathcal{N}(0,1)$, we can write

$$vNMSE\leqslant\mathbb{E}\left[\left(Z-\widehat{Z}\right)^2\right]+O\left(\sqrt{\frac{\log d}{d}}\right)\,.\quad\square$$

C Derivation of Equations for Algorithm 2

As we described in §3.4 through an example, and as illustrated by Figure 1, we have found through examining the solver's solutions, for our parameter range, that the optimal approach for the client has a structure that we can generalize. This allows us to readily interpolate the algorithm to non-quantile values $Z\notin\mathcal{Q}_m$ without stochastically quantizing the coordinate to a quantile.

	$x=0$	$x=1$	$x=2$	$x=3$
$h=0$	-5.48	-1.23	**0.164**	1.68
$h=1$	-3.04	-0.831	**0.490**	2.18
$h=2$	-2.18	**-0.490**	0.831	3.04
$h=3$	-1.68	**-0.164**	1.23	5.48

Recall the example from §3.4 with $\ell = b = 2$. There, we had the server table:

When $Z = 0$, the client would send $X = 2$ if $H \leqslant 1$ and $X = 1$ otherwise, leading to $\mathbb{E}\left[\widehat{Z}\right] = 0$. Now consider $Z = 0.1$; the client can increase the expected server's estimate by changing its behaviour for the leftmost and then uppermost cell, namely $X = 1, H = 2$. Specifically, by following

$$S''_x(H, 0.1) \approx \begin{cases} 1 & \text{If } (x = 2 \wedge H \leqslant 1) \vee (x = 1 \wedge H = 3) \\ 0.3 & \text{If } (x = 1 \wedge H = 2) \\ 0.7 & \text{If } (x = 2 \wedge H = 2) \\ 0 & \text{Otherwise} \end{cases} ,$$

In general, by applying the monotonicity constraints[5] we observed a common pattern in the optimal solution found by the solver for any b and ℓ (in the range we tested). Namely, when the server table is monotone, the optimal solution *deterministically* selects the message to send in all but (at most) one shared randomness value. For example, S''_x above deterministically selects the message if $H \neq 2$ (sending 1 if $H = 3$ and 2 if $H \in \{0, 1\}$) and stochastically selects between $x = 1$ and $x = 2$ when $H = 2$. Furthermore, the shared randomness value in which we should stochastically select the message is easy to calculate. Specifically, let $\underline{x}(Z) \in \mathcal{X}_b$ denote the maximal value such that sending $\underline{x}(Z)$ for all H would result in not overestimating Z in expectation (that is: $\underline{x}(Z) = \max\left\{x \in \mathcal{X}_b \mid \frac{1}{2^\ell} \cdot \sum_{h \in \mathcal{H}_\ell} r_{h,x} \leqslant Z\right\}$). We note that there must exists such a $\underline{x}(Z)$ because, by design, the solver's output for the optimal solution would always satisfy that $\frac{1}{2^\ell} \cdot \sum_{h=0}^{2^\ell} r_{h,0} = -T$ and $\frac{1}{2^\ell} \cdot \sum_{h=0}^{2^\ell} r_{h,2^b-1} = T$. (Otherwise, the solution would either be infeasible or suboptimal.) In particular, this means that we get $\underline{x}(Z) \in \mathcal{X}_b \backslash \left\{2^b - 1\right\}$ for all $Z \in [-T, T)$.

Next, let $\underline{h}(Z) \in \mathcal{H}_\ell$ denote the maximal value for which sending $\underline{x}(Z) + 1$ for all $H < \underline{h}$ and $\underline{x}(Z)$ for $H \geqslant \underline{h}$ would underestimate Z in expectation (for convenience, we consider $r_{2^b,h} = \infty$, for all $h \in \mathcal{H}_\ell$). Formally:

$$\underline{h}(Z) = \max\left\{ h \in \mathcal{H} \;\middle|\; \frac{1}{2^\ell} \cdot \left(\sum_{h'=0}^{h-1} r_{h',\underline{x}(Z)+1} + \sum_{h'=h}^{2^\ell-1} r_{h',\underline{x}(Z)} \right) \leqslant Z \right\} .$$

For example, consider $Z = 0.1$ in the $b = \ell = 2$ example above. We have that $\underline{x}(0.1) = 1$ since $\frac{1}{2^2} \cdot \sum_{h \in \mathcal{H}_2} r_{h,1} \leqslant 0.1$ and $\frac{1}{2^2} \cdot \sum_{h \in \mathcal{H}_2} r_{h,2} > 0.1$. We also have that $\underline{h}(Z) = 2$ as $\frac{1}{4} \cdot (0.164 + 0.49 + (-0.49) + (-0.164)) \leqslant 0.1$ and $\frac{1}{4} \cdot (0.164 + 0.49 + 0.831 + (-0.164)) > 0.1$. Similarly, for $Z = 3$ we get $\underline{x}(3) = 2$ and $\underline{h}(3) = 3$.

The interpolated algorithm works as follows: If $H < \underline{h}$, it deterministically sends $\underline{x}(Z) + 1$, i.e., $S_x(H, Z) = \begin{cases} 1 & \text{If } (x = \underline{x}(Z) + 1) \\ 0 & \text{otherwise} \end{cases}$. If $H > \underline{h}$, it sends $\underline{x}(Z)$, i.e., $S_x(H, Z) = \begin{cases} 1 & \text{If } (x = \underline{x}(Z)) \\ 0 & \text{otherwise} \end{cases}$. Finally, for $H = \underline{h}$, it stochastically selects between $\underline{x}(Z)$ and $\underline{x}(Z) + 1$. However, notice that the expected value of this quantization (given that $H = \underline{h}$) may *not* be exactly Z. Namely, as the algorithm needs to satisfy $\mathbb{E}[\widehat{Z} \mid Z] = \frac{1}{2^\ell} \sum_{h \in \mathcal{H}_\ell} \mathbb{E}[\widehat{Z} \mid H = h] = Z$, we require that

$$\mu \triangleq \mathbb{E}[\widehat{Z} \mid H = \underline{h}] = 2^\ell \cdot Z - \sum_{h=0}^{\underline{h}-1} r_{h,\underline{x}(Z)+1} + \sum_{h=\underline{h}+1}^{2^\ell-1} r_{h,\underline{x}(Z)} .$$

Knowing the desired expectation, the overall client's algorithm is then defined as:

$$S_x(H,Z) = \begin{cases} 1 & \text{If } (x = \underline{x}(Z) \wedge H > \underline{h}) \vee (x = \underline{x}(Z)+1 \wedge H < \underline{h}) \\ \frac{\mu - r_{h,\underline{x}(Z)}}{r_{h,\underline{x}(Z)+1} - r_{h,\underline{x}(Z)}} & \text{If } (x = \underline{x}(Z)+1 \wedge H = \underline{h}) \\ \frac{r_{h,\underline{x}(Z)+1} - \mu}{r_{h,\underline{x}(Z)+1} - r_{h,\underline{x}(Z)}} & \text{If } (x = \underline{x}(Z) \wedge H = \underline{h}) \\ 0 & \text{Otherwise} \end{cases} . \tag{9}$$

Indeed, by our choice of μ, the algorithm is guaranteed to be unbiased for all $Z \in [-T,T]$. This gives the final algorithm, whose pseudo-code appears in Algorithm 2. As in Algorithm 1, each client c rotates its vector and scales it by $\frac{\sqrt{d}}{\|x_c\|_2}$ to get a vectors whose coordinates' distribution approach i.i.d. $\mathcal{N}(0,1)$. Next, for each entry $\overline{Z}_c[i]$ the client computes $\underline{x}(\overline{Z}_c[i]), \underline{h}(\overline{Z}_c[i])$, and then it computes $S(H_c, \overline{Z}_c[i])$ as shown in Eq (9). Finally, it samples a message for each coordinate $\overline{X}_c \sim S(H_c, \overline{Z}_c[i])$ that it sends to the server together with the norm $\|x_c\|_2$.

D Performance of QUIC-FL with the Randomized Hadamard Transform

As described earlier, while ideally we would like to use a fully random rotation on the d-dimensional sphere as the first step to our algorithms, this is computationally expensive. Instead, we suggest using a randomized Hadamard transform (RHT), which is computationally more efficient. We formally show below that we maintain some performance bounds using a single RHT.

We note that some works suggest using two or three successive randomized Hadamard transforms to obtain something that should be closer to a uniform random rotation [63, 64]. This naturally takes more computation time. In our case, and in line with previous works [5, 7], we find empirically that one RHT appears to suffice. Unlike these works, our algorithm remains provably unbiased and maintains strong $NMSE$ guarantees in this case. Determining better provable bounds using two or more RHTs is left as an open problem.

Theorem 2. *Let $x \in \mathbb{R}^d$, let $\mathcal{R}_{RHT}(x)$ be its randomized Hadamard transform, and let $\mathfrak{Z} = \frac{\sqrt{d}}{\|x\|_2}\mathcal{R}_{RHT}(x)[i]$ be a coordinate in the transformed vector. For any p, $\Pr[\mathfrak{Z} \notin [-T_p, T_p]] \leqslant 3.2p$.*

Proof. Follows from the following theorem.

Theorem 3 ([65])**.** *Let $\epsilon_1, \ldots, \epsilon_d$ be i.i.d. Radamacher random variables and let $a \in \mathbb{R}^d$ such that $\|a\|_2^2 \leqslant 1$. For any $t \in \mathbb{R}$, $\Pr\left[\sum_{i=1}^{d} a_i \cdot \epsilon_i \geqslant t\right] \leqslant \frac{\Pr[Z \geqslant t]}{4\Pr[Z \geqslant \sqrt{2}]} \approx 3.1787 \Pr[Z \geqslant t]$, for $Z \sim \mathcal{N}(0,1)$.* □

Theorem 4. *Fix $p = \frac{1}{512}$; let $x \in \mathbb{R}^d$, let $\mathcal{R}_{RHT}(x)$ be its randomized Hadamard transform, and let $\mathfrak{Z} = \frac{\sqrt{d}}{\|x\|_2}\mathcal{R}_{RHT}(x)[i]$ be a coordinate in the transformed vector. Denoting by $E_b = \mathbb{E}\left[(\mathfrak{Z} - \widehat{\mathfrak{Z}_b})^2\right]$ the mean squared error using b bits per coordinate, we have $E_1 \leqslant 4.831$, $E_2 \leqslant 0.692$, $E_3 \leqslant 0.131$, $E_4 \leqslant 0.0272$.*

Proof. We present an approach to bound the MSE of encoding the coordinate $\mathfrak{Z}$, leveraging Theorem 3. Since we believe that it provides only a loose bound, we do not optimize the argument beyond showing the technique. Since the MSE, as a function of $\mathfrak{Z}$, is symmetric around 0 (as illustrated in Figure 7), we analyze the $\mathfrak{Z} \geqslant 0$ case.

The first option is to split $[0,T]$ into intervals, e.g., $I_1 = [0, 1.5]$, $I_2 = (1.5, 2.2]$, $I_3 = (2.2, T)$. Using Theorem 3, we get that $P_1 \triangleq \Pr[\mathfrak{Z} \notin [0,1.5]] \leqslant 3.2\Pr[Z \notin [0,1.5]] \leqslant 0.427$ and similarly, $P_2 \triangleq \Pr[\mathfrak{Z} \notin [0,2.2]] \leqslant 3.2\Pr[Z \notin [0,2.2]] \leqslant 0.089$. Next, we provide the maximal error for each bit budget b and such interval:

	$b=1$	$b=2$	$b=3$	$b=4$
$[0, 1.5]$	2.063	0.267	0.056	0.0134
$[1.5, 2.2]$	6.39	0.67	0.128	0.0285
$[2.2, T]$	16.73	3.51	0.617	0.11

Table 3: For each interval I and bit budget b, the maximal MSE, i.e., $\max_{z \in I} \mathbb{E}\left[(z - \widehat{z})^2\right]$.

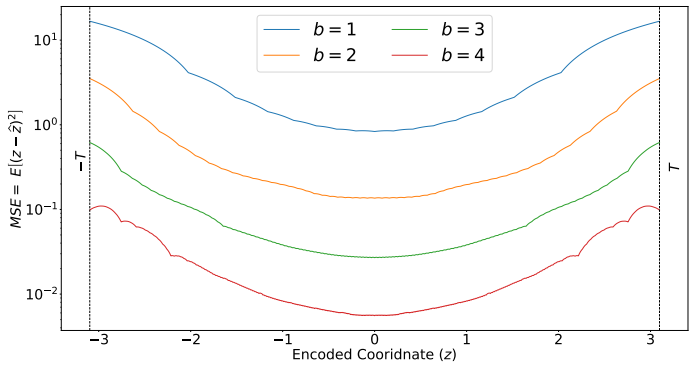


Figure 7: Expected squared error as a function of the value of $\mathfrak{Z}$ (for $p = \frac{1}{512}, m = 512$).

Note that for any $b \in \{1, 2, 3, 4\}$, the MSEs in I_3 are strictly larger than those in I_2 which are strictly larger than those in I_1. This allows us to derive formal bounds on the error. For example, for $b = 1$, we have that the error is bounded by

$$E_1 \leqslant (1 - 0.427) \cdot 2.063 + (0.427 - 0.089) \cdot 6.39 + 0.089 \cdot 16.73 \leqslant 4.831.$$

Repeating this argument, we also obtain:

$$E_2 \leqslant (1 - 0.427) \cdot 0.267 + (0.427 - 0.089) \cdot 0.67 + 0.089 \cdot 3.51 \leqslant 0.692$$
$$E_3 \leqslant (1 - 0.427) \cdot 0.056 + (0.427 - 0.089) \cdot 0.128 + 0.089 \cdot 0.617 \leqslant 0.131$$
$$E_4 \leqslant (1 - 0.427) \cdot 0.0134 + (0.427 - 0.089) \cdot 0.0285 + 0.089 \cdot 0.11 \leqslant 0.0272. \qquad \square$$

E Shakespeare Experiments details

The Shakespeare next-word prediction task was first suggested in [1] to naturally simulate a realistic heterogeneous federated learning setting. Its dataset consists of 18,424 lines of text from Shakespeare plays [22] partitioned among the respective 715 speakers (i.e., clients). We train a standard LSTM recurrent model [66] with $\approx 820K$ parameters and follow precisely the setup described in [24] for the Adam server optimizer case. We restate the hyperparameters for convenience in Table 4.

Task	Clients per round	Rounds	Batch size	Client lr	Server lr	Adam's ϵ
Shakespeare	10	1200	4	1	10^{-2}	10^{-3}

Table 4: Hyperparameters for the Shakespeare next-word prediction experiments.

F Additional Evaluation

F.1 Distributed Power Iteration

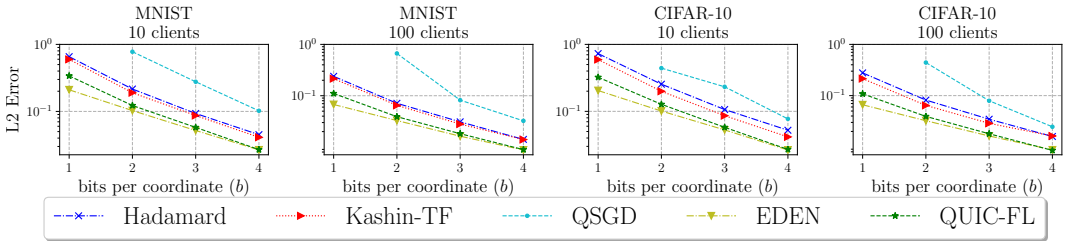


Figure 8: Distributed power iteration of MNIST and CIFAR-10 with 10 and 100 clients.

We simulate 10 clients that distributively compute the top eigenvector in a matrix (i.e., the matrix rows are distributed among the clients). Particularly, each client executes a power iteration, compresses its

top eigenvector, and sends it to the server. The server updates the next estimated eigenvector by the averaged diffs (of each client to the eigenvector from the previous round) and scales it by a learning rate of 0.1. Then, the estimated eigenvector is sent by the server to the clients and the next round can begin.

Figure 8 presents the L2 error of the obtained eigenvector by each compression scheme when compared to the eigenvector that is achieved without compression. The results cover bit budget b from one bit to four bits for both MNIST and CIFAR-10 [25, 29, 30] datasets. Each distributed power iteration simulation is executed for 50 rounds for the MNIST dataset and for 200 rounds for the CIFAR-10 dataset.

As shown, QUIC-FL has an accuracy that is competitive with that of EDEN (especially for $b \geqslant 2$), and considerably better than other algorithms that offer fast decoding time. Also, Kashin-TF is not unbiased (as illustrated by Figure 2), and is therefore less competitive for a larger number of clients.

F.2 Federated Learning: Extended comparison with QSGD

We repeat the experiments from Figure 5 and Figure 6, adding another curve for QSGD, which uses twice the bandwidth of the other algorithms (one bit for sign, and another for the stochastic quantization). As shown in figures 9 and 10, even with the additional bandwidth, QSGD's accuracy is lower than all algorithms except CS. We note that QSGD also has a more accurate variant that uses variable length encoding [14]. However, it is not GPU-friendly, and therefore, as with other variable length encoding schemes as we have discussed previously, we do not include it in the experiment.

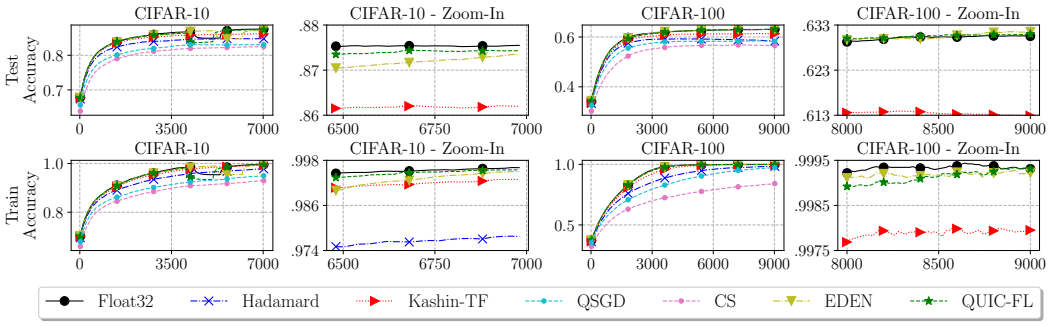


Figure 9: Train and test accuracy for CIFAR-10 and CIFAR-100 with 10 persistent clients (i.e., silos) and $b = 1$.

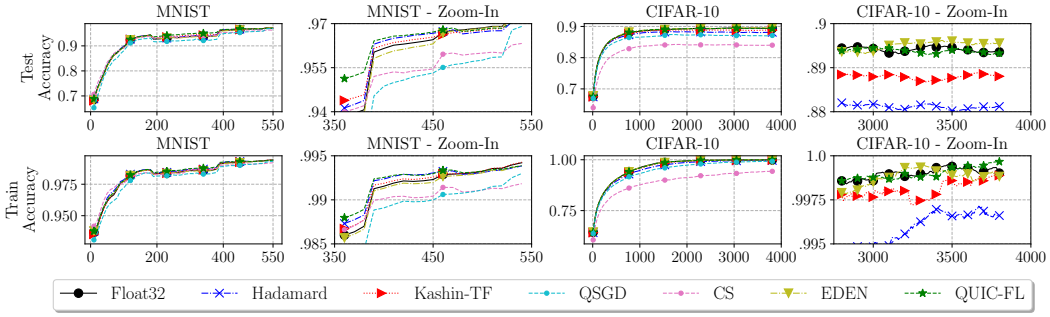


Figure 10: Cross-device federated learning of MNIST and CIFAR-10 with 50 clients and $b = 1$.